Results in Physics 9 (2018) 1481–1493

Contents lists available at ScienceDirect

Results in Physics

journal homepage: www.elsevier.com/locate/rinp

Experimental and quantum chemical studies of functionalized tetrahydropyridines as corrosion inhibitors for mild steel in 1 M hydrochloric acid

Jiyaul Haque[a], Chandrabhan Verma[b,c,*], Vandana Srivastava[a], M.A. Quraishi[a,d,*], Eno E. Ebenso[b,c,*]

[a] Department of Chemistry, Indian Institute of Technology, Banaras Hindu University, Varanasi 221005, India
[b] Department of Chemistry, Faculty of Natural and Agricultural Sciences, School of Chemical and Physical Sciences, North-West University, Private Bag X2046, Mmabatho 2735, South Africa
[c] Material Science Innovation & Modelling (MaSIM) Research Focus Area, Faculty of Natural and Agricultural Sciences, North-West University, Private Bag X2046, Mmabatho 2735, South Africa
[d] Center of Research Excellence in Corrosion, Research Institute, King Fahd University of Petroleum and Minerals, Dhahran 31261, Saudi Arabia

ARTICLE INFO

Keywords:
Mild steel
Acid solution
Corrosion inhibition
Tetrahydropyridines (THPs)
Quantum chemical calculations

ABSTRACT

Corrosion inhibition property of ethyl 1,2,6-triphenyl-4-(phenylamino)-1,2,5,6-tetrahydropyridine-3-carboxylate (THP-1) and ethyl 2,6-bis(4-methoxyphenyl)-1-phenyl-4-(phenylamino)-1,2,5,6-tetrahydropyridine-3-carboxylate (THP-2) on mild steel (MS) in 1 M HCl have been studied using weight loss, electrochemical, surface morphology (SEM, AFM) and quantum chemical (QC) calculations methods. Results showed that both the functionalized tetrahydropyridines act as an excellent inhibition for mild steel (MS) and it exhibited the maximum inhibition efficiency (IE) of 90.67% (THP-1) and 94.30% (THP-2) at 7.95×10^{-5} M concentration. Results further showed that adsorption of THPs on metallic surface obeyed the Langmuir adsorption isotherm. Potentiodynamic polarization (PDP) study revealed that studied compounds acted as mixed type inhibitors. Electrochemical impedance spectroscopy (EIS) study suggests that the investigated inhibitors inhibit corrosion by adsorbing at the metal/electrolyte interfaces. The SEM, EDX and AFM studies showed that the THPs form a protective covering over the metallic surface that isolates the metal from aggressive acid solution and thereby protect form corrosive dissolution. Quantum chemical (QC) calculations carried out using DFT methods for neutral, solvated and protonated forms of inhibitors provides reasonable support to the experimental findings.

Introduction

Mild steel is a low carbon steel alloy (0.05–0.25% carbon) which is widely used as constructional resource in several industries including petroleum, food, power production, chemical industries because of its high mechanical strength, easy fabrication and low cost [1,2]. However, the mild steel is very susceptible to corrosion and readily undergoes corrosive dissolution during several common industrial processes such as etching, acid pickling, acid descaling and acid cleaning and oil well acidification [3]. Literature survey reveals that several types of corrosion inhibitors have been used previously to mitigate the metallic corrosion. Among them, the use of organic inhibitors has gained the highest priority due to their ease synthesis at low cost and high protection ability. The organic compounds containing heteroatoms (N, O, S and P) and π-electrons have proved by experimental as well as theoretically act as effectively corrosion inhibitors in a wide range of acid solution through the adsorption on the metal surface and blocking the active corrosion sites. Through their adsorption, these inhibitors form a protective film between the corrosive media and metallic surface and retard the metal dissolution in acid solution [4–7]. However, most of the well-known reported corrosion inhibitors are toxic and non-environmental friendly because of their traditional synthesis using multistep reactions. However, recently increasing demands of green chemistry and strict environmental rules and accidental news have restricted their use in industrial applications. Therefore, the current research focused on the design of green corrosion inhibitors, which are not harmful to the environment [8,9]. The multicomponent reactions (MCRs) have immersed as a potential tool for green synthesis for

* Corresponding authors at: Department of Chemistry, Faculty of Natural and Agricultural Sciences, School of Chemical and Physical Sciences, North-West University, Private Bag X2046, Mmabatho 2735, South Africa (C. Verma). Department of Chemistry, Indian Institute of Technology, Banaras Hindu University, Varanasi 221005, India (M.A. Quraishi and E.E. Ebenso).
E-mail addresses: chandraverma.rs.apc@itbhu.ac.in (C. Verma), maquraishi.apc@itbhu.ac.in (M.A. Quraishi), Eno.Ebenso@nwu.ac.za (E.E. Ebenso).

https://doi.org/10.1016/j.rinp.2018.04.069
Received 5 March 2018; Received in revised form 27 April 2018; Accepted 28 April 2018
Available online 08 May 2018

organic compounds possess industrial and biological activities [10,11]. These MCRs have several advantages including simple handling, good atom economy and minimum waste generation, and simple work-up process [12,13]. Literature survey reveals that the functionalized tetrahydropyridines (THPs) are an essential building block for numerous natural products, pharmaceuticals and a wide variety of biologically active compounds [14].

In view of the above, present study deals with the synthesis and corrosion inhibition performance of two tetrahydropyridines (THP-1 and THP-2) on mild steel corrosion in 1 M HCl using chemical (Weight loss), electrochemical (EIS and PDP) and DFT methods. As per the best of our knowledge, the investigated tetrahydropyridines (THP-1 and THP-2) is being utilized for the first time as corrosion inhibitors. The selection of these compounds as corrosion inhibitors is because they contain N and O atoms in the form of polar functional moieties and various π-electrons through which they can easily adsorb and inhibit corrosion efficiently. Moreover, the investigated tetrahydropyridines (THP-1 and THP-2) have been synthesized using the MCRs that offer green and environmental benign protocol. Additionally, the starting materials used in the synthesis of THPs are easily available and LD_{50} values are more than 250 mg/kg bw for rate which further suggests that investigated tetrahydropyridines (THP-1 and THP-2) are green chemicals to be tested as corrosion inhibitors.

Experimental section

Inhibitors synthesis (THPs)

The corrosion inhibitors used in the study were synthesized by previously described by Wang et al. [15]. Scheme for the synthesis of inhibitors is given in Fig. 1 and informations related to the molecules such as chemical structures, melting point, IUPAC nomenclature are summarized in Table 1. Theeir FT-IR and 1H NMR spectra are given in Fig. S1.

Materials and test solution

For weight loss, electrochemical and SEM/, EDX and AFM analyses mild steel specimens having chemical composition of (%wt) C 0.076%, Si 0.026%, Mn 0.192, P 0.012%, Cr 0.050%, Ni 0.050%, Al 0.023%, Cu 0.135% and remaining Fe were employed. Surface pretreatment for the MS sample preparation for all experiments was carried out by previously reported method [16]. The corrosive 1 M HCl solution was prepared by the dilution of analytical grade 37% HCl with double-distilled water (Fig. 2).

Weight loss measurement

The weight loss measurement has been carried out on the MS specimens of the above-mentioned chemical composition by the previously described method [17]. The *IE*, surface coverage (θ) and corrosion rate (C_R), were calculated by the following equations:

$$C_R = \frac{W}{At} \tag{1}$$

$$IE\ (\%) = \frac{C_R - C_{R(i)}}{C_R} \times 100 \tag{2}$$

$$\theta = \frac{C_R - C_{R(i)}}{C_R} \tag{3}$$

where C_R and $C_{R(i)}$ are the corrosion rate in the absence and presence of inhibitors, respectively. t is the exposure time (h), W and A are weight loss (mg) and area (cm^2) of the specimen, respectively.

Electrochemical measurement

Electrochemical experiments have been performed by using a standard three electrode-electrochemical glass-cell consisting of the working electrode (mild steel), a counter electrode (platinum foil) and a reference electrode (saturated calomel electrode; SCE), as described previously [18]. The EIS was performed at open circuit potential with amplitude 10 mV peak to peak in the frequency range of 100 kHz to 0.01 Hz. The charge transfers resistance (R_{ct}) was derived from the Nyquist plots. The corrosion *IE* was calculated by the following formula:

$$IE\ (\%) = \frac{R_p^i - R_p^0}{R_p^i} \times 100 \tag{4}$$

where R_p^0 and R_p^i are the polarization resistance in the presence and absence of THPs, respectively.

The PDP experiment was carried out on the MS specimen by changing the electrode potential from −0.25 to +0.25 V versus corrosion potential (E_{corr}) at 1.0 mV s^{-1} scan rate. The corrosion current density and other relevant parameters were calculated by fitting the linear segment of cathodic and anodic Tafel slopes. The IE was calculated from the corrosion current density through the following relationship:

$$\eta\ (\%) = \frac{i_{corr}^0 - i_{corr}^i}{i_{corr}^0} \times 100 \tag{5}$$

where the i_{corr}^0 and i_{corr}^i are the corrosion current density in the absence and presence of THPs, respectively.

Surface study

Surface morphology studies (SEM, EDX and AFM) performed by the method reported earlier [19]. Freshly prepared specimens of MS were immersed in 1 M HCl solution in the presence and absence of THPs. The specimens were taken out after 3 h. Then washed with distilled water and dried before surface analyses. Scanning electron microscope (SEM-EDX), Ziess Evo 50 XVP was used to analyze the changes occurs on metal surface along with the elemental composition using EDX analysis. The SEM images were taken at 1000x magnification. Atomic force microscopy (AFM), NT-MDT multimode AFM, Russia, 111, was used to capture images micrograph.

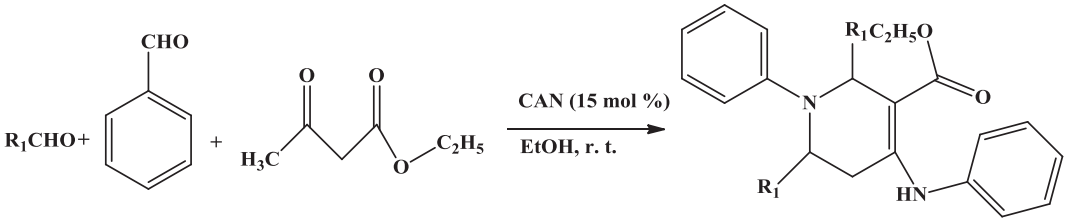

THP-1 R_1 = Ph
THP-2 R_1 = p-OCH_3Ph

Fig. 1. Synthetic route of studied THPs.

Table 1
IUPAC name, molecular structure, molecular formula, melting point and IR spectral data of THPs.

S. No.	IUPAC name and abbreviation of Inhibitor	Chemical Structure	Molecular formula and M.P
1	Ethyl 1,2,6-triphenyl-4-(phenylamino)-1,2,5,6-tetrahydropyridine-3-corboxlate (THP-1)	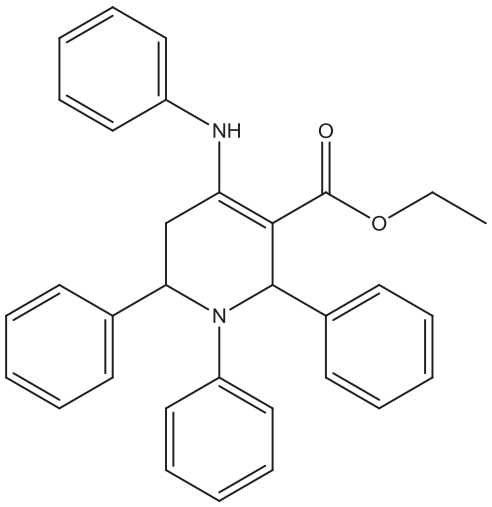	$C_{32}H_{30}N_2O_2$ (mol. wt. 474.60) M.P. 174 °C IR ν_{max}/cm^{-1} = 1446, 1483 (C=C), 1604 (Conjugated C=O), 2933 (C–N)
2	Ethyl 2,6-bis(4-methoxyphenyl)-1-phenyl-4-(phenylamino)-1,2,5,6-tetrahydropyridine-3-corboxylate (THP-2)	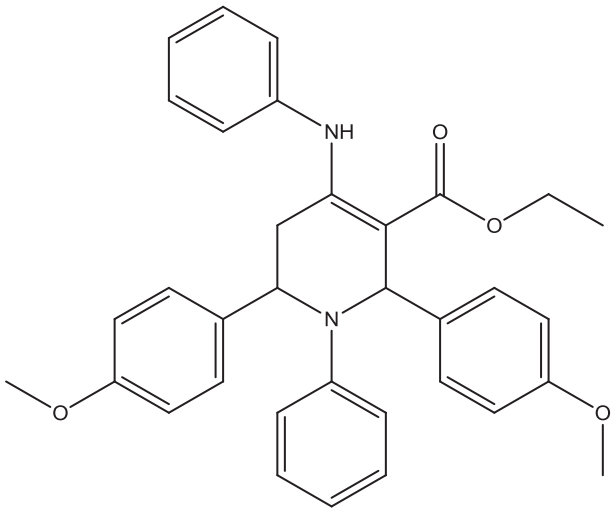	$C_{34}H_{34}N_2H_4$ (mol. Wt. 534.66) M.P. 181 °C IR ν_{max}/cm^{-1} = 1380, 1500 (C=C), 1600 (Conjugated C=O), 3225 (C–N).

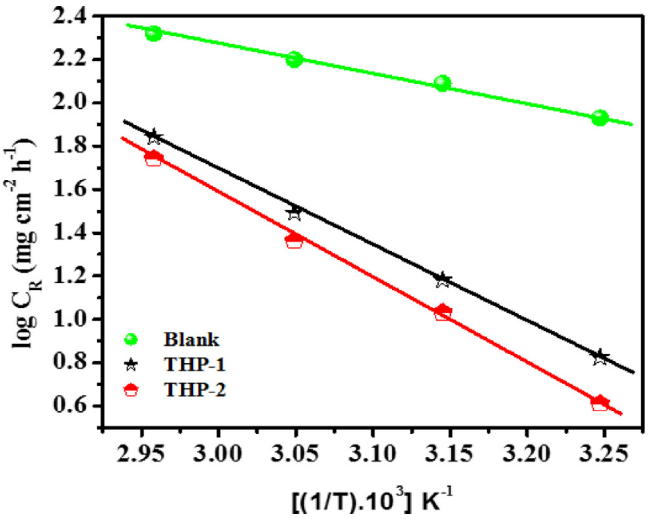

Fig. 2. Arrhenius plots for the corrosion rate of mild steel versus the temperature in 1 M HCl.

DFT study

DFT based QC calculation on the studies inhibitor molecules was performed using the density functional theory (DFT). The B3LYP/6-13 G (d, p) basis set in Gaussian 09 package program was used for the DFT calculations in their neutral and protonated in gaseous as well as aqueous phases [7,20]. The integral equation formalism polarizable continuum model (IEFPCM) was used to analyze the effect of water molecules on the geometry and electronic parameters of THPs. Then, several QC parameters such as frontier molecular orbital (FMO), that is highest occupied molecular energy (E_{HOMO}) and lowest unoccupied molecular energy (E_{LUMO}) and other derivative quantities were calculated by the optimized molecules. Energy gap ΔE, hardness (η) softness (σ), and electronegativity (χ) and fraction of electrons transfer (ΔN) parameters have been also derived by using the following equations:

$$\Delta E = E_{LUMO} - E_{HOMO} \quad (6)$$

$$\eta = \frac{1}{2}(E_{LUMO} - E_{HOMO}) \quad (7)$$

$$\sigma = \frac{1}{\eta} \quad (8)$$

$$\chi = -\frac{1}{2}(E_{LUMO} - E_{HOMO}) \quad (9)$$

$$\Delta N = \frac{\varphi - \chi_{inh}}{2(\eta_{Fe} + \eta_{inh})} \quad (10)$$

The fraction of electron transfers (ΔN) was calculated by using the equation 10, in which, work function (φ) was used in place of electronegativity of iron (χ_{Fe}), previously described [21,22]. Where η_{Fe} and η_{in} are the hardness of iron and inhibitor, respectively. For calculation of ΔN, ϕ value 4.82 was used, which is derived from the DFT calculation for the iron surface having highly stabilized energy and packed structure i.e., Fe(1 1 0) and the hardness of bulk iron was approximated to 0.0 eV/mol based on Pearson's electronegativity scale [23,24]. The positive value of ΔN (i.e., $\Delta N > 0$) indicates the electron transfer from the inhibitor to metal and vice versa [25].

The electrophilicity index (ω) introduced by the Parr et al. [26] and it is calculated by the following equation:

$$\omega = \frac{\mu^2}{4\eta} = \frac{\chi^2}{4\eta} \quad (11)$$

The nucleophilicity (N^0) is inverse of electrophilicity:

$$N^0 = \frac{1}{\omega} \quad (12)$$

Results and discussions

Weight loss experiment

Effect of concentration

Because weight loss is a simple, easy and reliable method, the corrosion inhibition performance of investigated tetrahydropyridine derivatives at different concentrations after 3 h immersion time in 1 M HCl test solution was first studied by this method. The effect of inhibitors concentrations on their corrosion inhibition efficiency is presented in Table. Results showed that that inhibition performance of both the studied inhibitors increases with their concentrations and maximum values were achieved at 7.95×10^{-5} M concentration. THP-1 and THP-2 showed the maximum IE of 90.67% and 94.30%, respectively. From the results, it is also clear that THP-2 exhibited higher IE as compared to THP-1 at all the studied concentrations. The higher IE of THP-2 than THP-1 is attributed due to +R effect (conjugation) of the two methoxy ($-OCH_3$) groups present on phenyl moiety [27]. The results given in Table 2 further showed that increased inhibitor concentration after 7.95×10^{-5} M did not show any significant enhancement in the inhibitors efficiency, which implies that at 7.95×10^{-5} M is optimum concentration.

Table 2
The weight loss parameters obtained for mild steel in 1 M HCl containing different concentration of THPs.

Inhibitors	Conc (M)	Weight loss (mg)	C_R (mg cm^{-2} h^{-1})	(θ)	*IE* (%)
Blank	0.00	193	6.43	–	–
THP-1	1.98×10^{-5}	116	3.86	0.3989	39.89
	3.97×10^{-5}	71	2.36	0.6321	63.21
	5.96×10^{-5}	41	1.36	0.7875	78.75
	7.95×10^{-5}	18	0.60	0.9067	90.67
	9.94×10^{-5}	17	0.56	0.9119	91.19
THP-2	1.98×10^{-5}	107	3.56	0.4455	44.55
	3.97×10^{-5}	57	1.90	0.7047	70.47
	5.96×10^{-5}	31	1.03	0.8393	83.93
	7.95×10^{-5}	11	0.36	0.9430	94.30
	9.94×10^{-5}	10	0.33	0.9481	94.81

Table 3
Variation of C_R and *IE* with temperature in absence and presence of optimum concentration of THPs in 1 M HCl.

Temperature (k)	Corrosion rate (C_R) (mg cm^{-2} h^{-1}) and inhibition efficiency (η%)					
	Blank		THP-1		THP-2	
	C_R	*IE* (%)	C_R	*IE* (%)	C_R	*IE* (%)
308	7.66	–	0.60	92.17	0.36	95.21
318	11.00	–	1.36	87.57	0.96	91.21
328	14.33	–	2.80	80.46	2.06	85.00
338	18.66	–	6.23	66.60	4.96	73.39

Effect of temperature

The temperature effect causes the effective change the inhibition performance of inhibitors. Therefore, we have tested the inhibition effect of 7.95×10^{-5} M concentration THPs inhibitor at the temperature range of 308–338 K. The variation of IE with solution temperature is summarized in Table 3. The results given in Table 3 showed that increased solution temperature resulted into decreased IE and increased corrosion rate (C_R), it may be due to desorption of inhibitors molecule occurs at higher temperature. Desorption of adsorbed inhibitor molecules form the metallic surface at elevated temperature, can results into the exposure of higher metallic surface area that will increase the corrosion rate. The activation energy (E_a) was calculated the Arrhenius equation as shown below [28]:

$$\log(C_R) = \frac{-E_a}{2.303RT} + \log A \quad (13)$$

where A is the Arrhenius pre-exponential factor, T is absolute temperature and R is the gas constant. The values of activation energies in absence and presence of inhibitors was derived from the slope values of Arrhenius plots (Fig. 3) and given in Table 4. The calculated values of E_a were 66.77 kJ mol^{-1} for THP-1 and 73.37 kJ mol^{-1} for THP-2, while in absence of inhibitor molecules it was only 38.48 kJ mol^{-1}. The increased values of activation energies in presence of both inhibitors as compare to in their absence indicate that more energy barrier has been achieved and corrosion process has become more difficult due to the formation of a protective film by the THPs molecule at metal- electrolyte interfaces [29,30]. Further, the higher values of E_a in the presence of THPs confirmed the electrostatic interaction between inhibitor molecules and metallic surface [31].

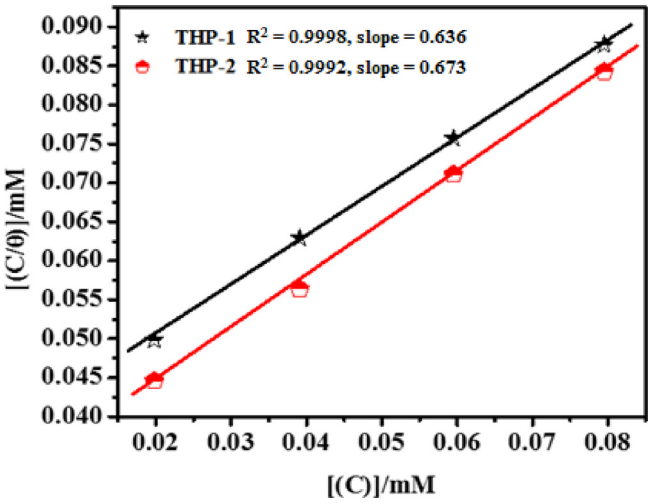

Fig. 3. Langmuir isotherm plots for the adsorption of THPs on mild steel surface in 1 M HCl.

Table 4
The value of k_{ads} and ΔG^0_{ads} for mild steel in absence and presence of optimum concentration of THPs in 1 M HCl at different studied temperature.

Inhibitors	K_{ads} (10^4 M^{-1})				$-\Delta G_{ads}$ (K J mol^{-1})			
	308	318	328	338	308	318	328	338
THP-1	1.41	0.84	0.49	0.23	34.76	34.53	34.15	33.16
THP-2	2.38	1.24	0.68	0.33	36.10	35.56	35.02	34.07

Adsorption isotherm

The adsorption isotherm is very essential to understand the adsorption mechanism of organic molecules on the metallic surface [32]. The study of adsorption isotherm gives information about structural properties of the electric double layer along with thermodynamic information. The Freundlich, Temkin and Langmuir adsorption isotherms were tested in the present study in order to find the best fit among which Langmuir isotherm was best fitted with the values of regression coefficient (R^2) close to one which validates the applicability of this approach, shown in Fig. 3 [27]. The values R^2 were 0.9996 and 0.9991 for THP-1 and THP-2 respectively. The Langmuir isothermal can be represented by following relationship [33].

$$\frac{C}{\theta} = \frac{1}{K_{ads}} + C \tag{14}$$

where K_{ads} is the adsorption–desorption constant processes occurring on the metal surface C is the molar concentration of THPs and θ is the degree of surface coverage of THPs inhibitor at MS surface. The values of K_{ads} were calculated at different temperatures from the intercept of the Langmuir isotherm plots. The standard free energy of adsorption (ΔG^0_{ads}) was calculated by using following equation:

$$\Delta G = -RT\ln(55.5K_{ads}) \tag{15}$$

In the above equation, the numerical value 55.5 is the molar concentration of water in hydrochloric acid solution. R and T are the universal gas constant and absolute temperature (in kelvin), respectively. The calculated values of K_{ads} and ΔG^0_{ads} are given in Table 4. Comparing with literatures, the ΔG^0_{ads} of studied inhibitors is more negative, indicates that adsorption of THPs on MS surface is more spontaneously [34–37].

The enthalpy of adsorption (ΔH) and entropy of adsorption (ΔS) were calculated by using the Gibbs-Helmholtz equation:

$$\Delta G_{ads} = \Delta H_{ads} - T\Delta S_{ads} \tag{16}$$

The plots between ΔG_{ads} verse T are given in Fig. S2. The values of ΔH_{ads} and ΔS_{ads} were calculated from intercept and slope of the plots, respectively. The obtained ΔH_{ads} value for THP-1 and THP-2 are -50.92 kJ mol^{-1} and -56.62 kJ mol^{-1}, respectively. The obtained ΔH_{ads} values of inhibitors indicated that the studied THP-1 and THP-2 adsorption is predominantly physical and exothermic in nurture [38].

Electrochemical measurements

PDP study

The Tafel polarization curves for the MS in 1 M HCl with and without THPs molecules at 7.95×10^{-5} M concentration are displayed in Fig. 4. The PDP parameters such as corrosion potential (E_{corr}), Tafel slop (β_a, β_c), corrosion current density (i_{corr}) obtained through the extrapolation of the linear segments of Tafel curves and *IE* was calculated by Eq. (5) from the obtained values of i_{corr}, are listed in Table 5. From the results (Table 5 and Fig. 4), it can be observed that the addition of THPs inhibitors in acidic solution decreases anodic as well as cathodic reactions. The Tafel curves for MS dissolution are similar in the presence and absence of inhibitor molecules suggesting that although the studied molecules inhibit corrosion but did not change its mechanism

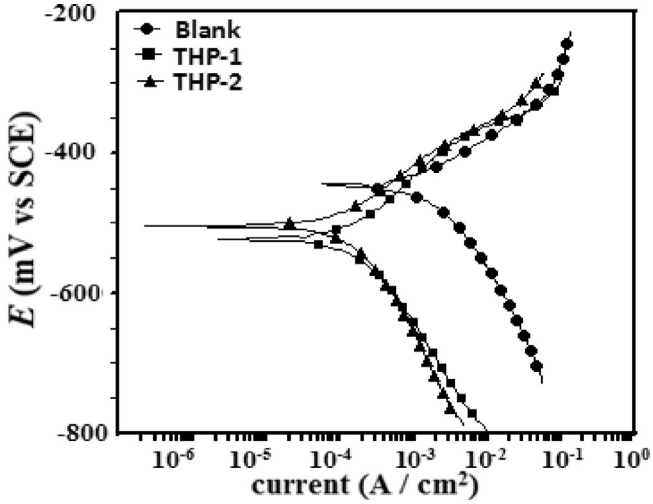

Fig. 4. Tafel curves for mild steel in 1 M HCl in absence and presence of optimum concentration of THPs at 308 K.

[39,40]. In presence of inhibitors, the maximum change in the value of E_{corr} was 77 mV which is less than 85 mV, which indicates that the studied compounds behave as mixed type inhibitors, and it affects both anodic oxidative metallic dissolution as well as cathodic reductive evolution of hydrogen reactions [41]. It is also observed that Tafel slope values (β_a and β_c) (Table 5) did not changed significantly in the presence of THP-1 and THP-2 which further suggest the THPs inhibit both the anodic and cathodic reactions and acted as mixed type corrosion inhibitors.

EIS study

EIS is another very helpful which provides additional information about the corrosion inhibition behavior of organic compounds on MS in acid solution. Fig. 5(a) and (b) are Nyquist and Bode plots of MS in 1 M HCl in the presence and absence of inhibitors. In Fig. 5(a) it can be seen that in the presence of THPs the diameters of Nyquist plot increase as compare to the blank, indicated that the formation of the protective film on the metal surface, which resulted into an increased value of the charge transfer resistance in presence of inhibitors. An appropriate equivalent circuit was using to extract the impedance data [Fig. 5(c)]. The equivalent circuit includes constant phase element (CPE), polarization resistance (R_p) and solution resistance (R_s). In absence of inhibitor, the polarization resistance (R^0_p) of mild steel in 1 M HCl solution is equal to the charge transfer resistance (R_{ct}) [42]. However, in addition of inhibitor molecule, the structure of metal solution interface changes due to the adsorption of inhibitor, therefore the polarization resistance (R^i_p) must be equal to the sum of R_{ct}, and R_f (film resistance) etc. (i.e. $R^i_p = R_{ct} + R_f$) [43]. In our present study, we used CPE in place of capacitance because it gives the superior estimation for the metal corroding in the acidic electrolytic solution [3,44]. The impedance of CPE can be defined as:

$$Z_{CPE} = Y_0^{-1}(j\omega)^{-n} \tag{17}$$

where ω is the angular frequency, j is the imaginary number ($j^2 = -1$), Y_0 is the amplitude comparable to a capacitance and n is the phase shift (exponent). The phase shift value gives information about the degree of metal surface inhomogeneity. The higher the n value is related to the lower surface roughness i.e., low surface inhomogeneity. The CPE can represent as resistance when $n = 0$, $Y_0 = R$), capacitance when n = 1 ($Y_0 = R$) and inductance when $n = -1$ ($Y_0 = 1/L$), or Warburg impedance when n = 0.5 ($Y_0 = W$) based on the value of n. The EIS parameters derived from Nyquist plots are given in Table 6. From the results (Table 6), it can be seen that the n values for THPs were between

Table 5
Tafel polarization parameters for mild steel in 1 M HCl in absence and presence of optimum concentration of THPs.

Inhibitors	Conc (M)	E_{corr} (mV/SCE)	β_a (mV/dec)	$-\beta_c$ (mV/dec)	i_{corr} (μA/cm^2)	*IE* (%)	θ	χ^2
Blank	–	−445	70.5	114.6	1150			1.12×10^{-3}
THP-1	7.96×10^{-5}	−522	122.8	161.3	133	88.43	0.8843	1.01×10^{-3}
THP-2	7.96×10^{-5}	−503	99.1	160.3	107	90.69	0.9069	1.43×10^{-3}

0.856 and 0.892, which are higher than the value of *n* for blank (0.827). From the results depicted in Table 6, it can be further seen that the surface inhomogeneity decrease in the presence of inhibitor, indicated that the formation of a protective film on the metal surface. In our present case, value of double layer capacitance (C_{dl}) was calculated by using the following equation [45] Table 7.

$$C_{dl} = -Y^0(\omega_{max})^{n-1} \quad (18)$$

where ω_{max} is the angular frequency at which the imaginary part of impedance has maximum [46–49]. From the table, the goodness (χ^2) of

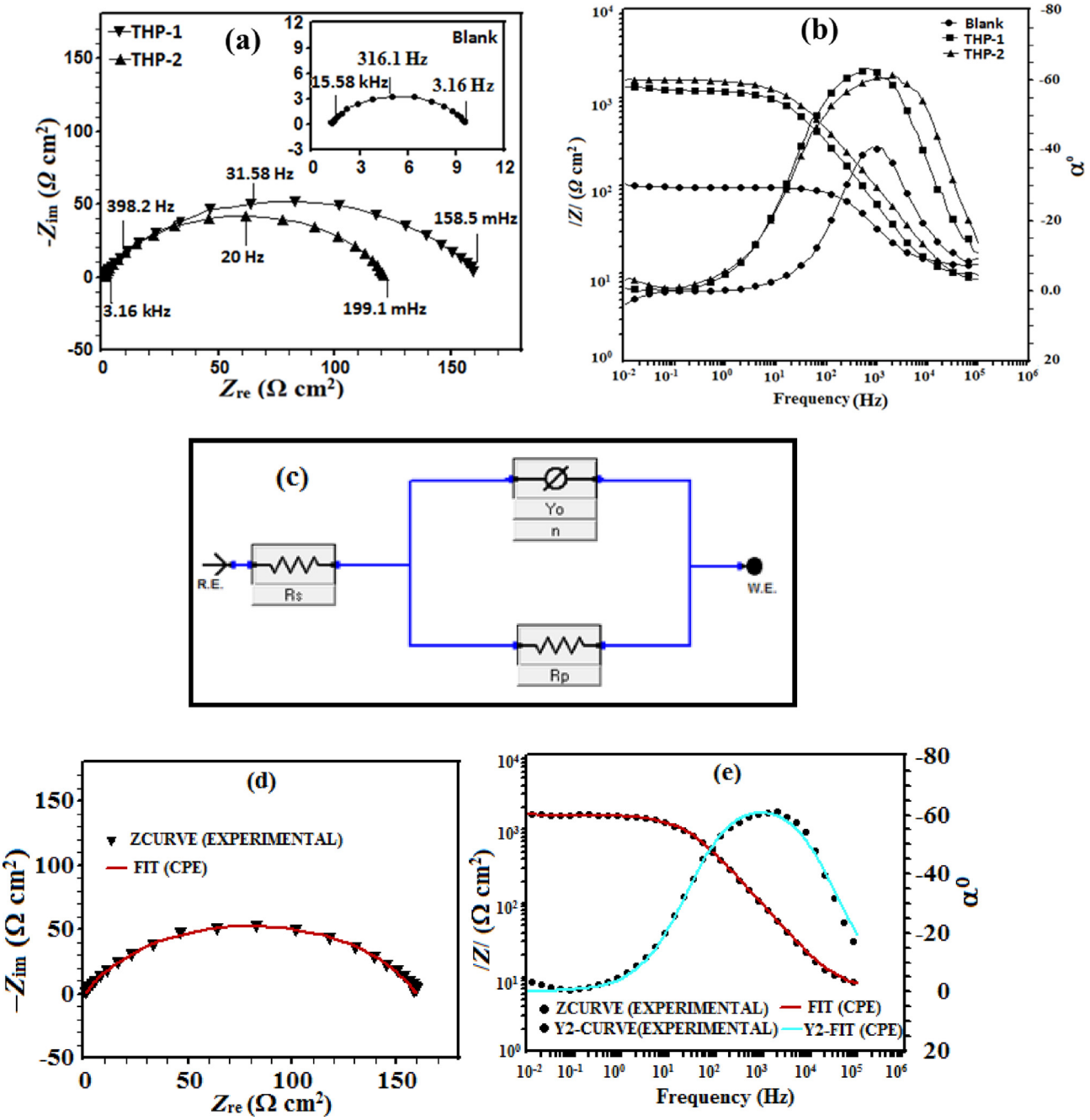

Fig. 5. (a) Nyquist plots and (b) Bode plots for mild steel in 1 M HCl in absence and presence of optimum concentration of THPs at 308 K, (c) Equivalent circuit used for fitting and a analyzing the electrochemical data and (d–e) fitted Nyquist and Bode plot for THP-2.

Table 6
The EIS parameters obtained for mild steel in 1 M HCl in absence and presence of optimum concentration of THPs.

Inhibitors	Conc (M)	R_S (Ω)	R_f (Ω cm^2)	R_P (Ω cm^2)	n	Y^0 (μF/cm^2)	C_{dl} (μF cm^{-2})	IE (%)	θ
	–	1.12	0.818	9.58	0.827	482.2	106.28	–	–
THP-1	7.95×10^{-5}	0.849	0.576	119.9	0.856	173.2	47.89	89.71	0.8971
THP-2	7.59×10^{-5}	0.664	0.455	157.5	0.892	149.2	33.50	92.19	0.9219

Table 7
Values of slope and phase angle for both inhibitors derived from Bode plot.

Inhibitors	Conc. (M)	Slope	Phase angle (α)
Blank	–	−0.48	−41.30
THP-1	7.95×10^{-5}	−0.69	−61.36
THP-2	7.95×10^{-5}	−0.73	−63.36

fit is very close to 10^{-3}, supported the validity of used circuit. The magnitude of R_p increases while the values of C_{dl} decreases in the presence of 7.95×10^{-5} M THPs molecule in 1 M HCl, which cause increase the *IE %* (Eq. 4), indicated that the THPs inhibit the corrosion of MS effectively. Decrease the C_{dl}, it may be due to either increase in the thickness of electric double layer or decrease in local dielectric constant or both which is consequence due to adsorption of THPs inhibitors on MS surface. The order of IE THP-2 > THP-1 followed the weight loss results.

Surface measurement

SEM/EDX analysis

The surface examinations of the inhibited and uninhibited metallic specimens give further insight about the inhibition behavior of the inhibitor molecules. The SEM images of inhibited and uninhibited MS specimens and their corresponding EDX spectra after immersion for 3 h in 1 M HCl are given in Figs. 6 and 7. Fig. 8 represents the SEM image of uninhibited MS specimen which shows a highly damaged and corroded specimens resulted due to free acid corrosion in absence of inhibitors. Moreover, the SEM image of the metallic specimen in without inhibitor shows some pits and cracks in addition to the mountain like appearance. However, from the SEM images in presence of THPs molecule, it can be seen the metallic surface become significantly smoothened which could be possible as a result of the formation of a protective layer by inhibitor molecules over the metallic surface. The inhibition performance of the studied compounds was further supported by their EDX spectral analysis. The EDX spectra of the metallic specimen in absence of inhibitors showed the signals only iron, carbon and oxygen. The signal for the presence of oxygen in the EDX spectrum of uninhibited solution which is indicated that the formation of the surface oxide layer

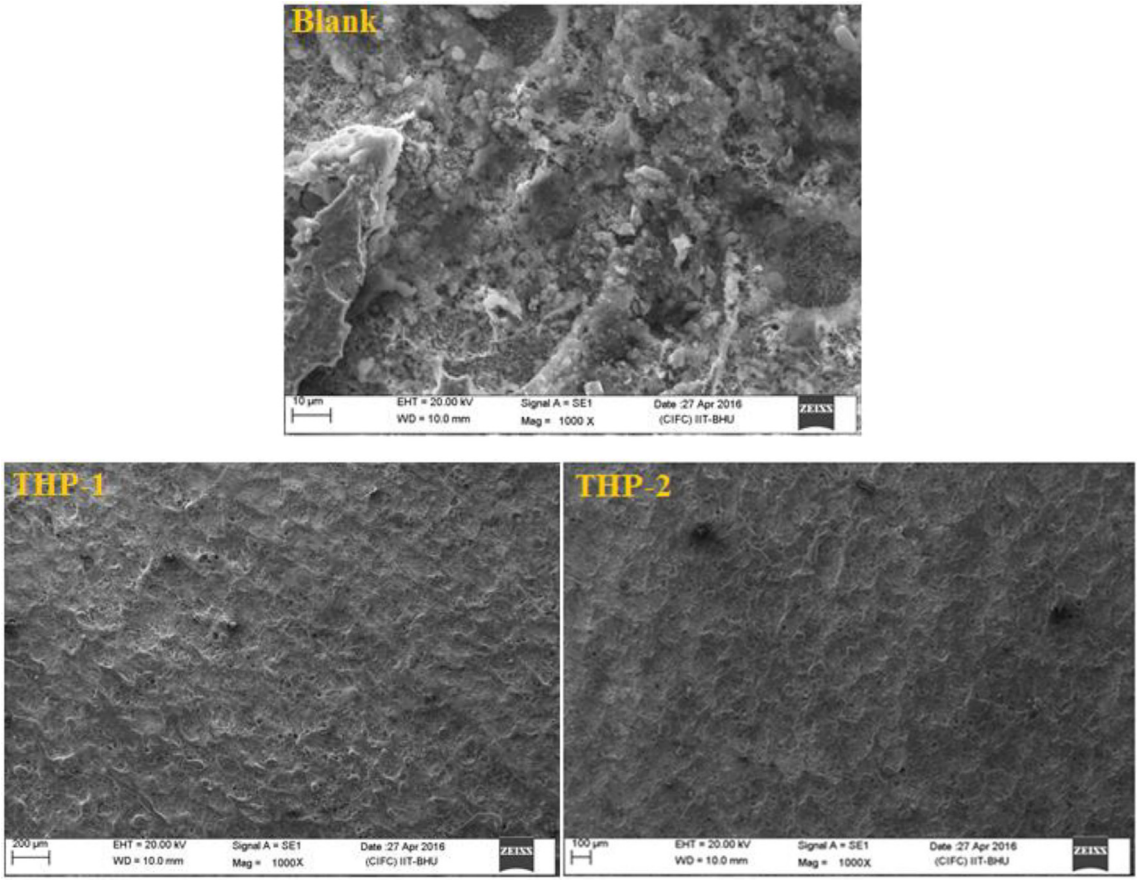

Fig. 6. SEM image of mild steel surface in absence and present of 40 ppm of THPs inhibitors.

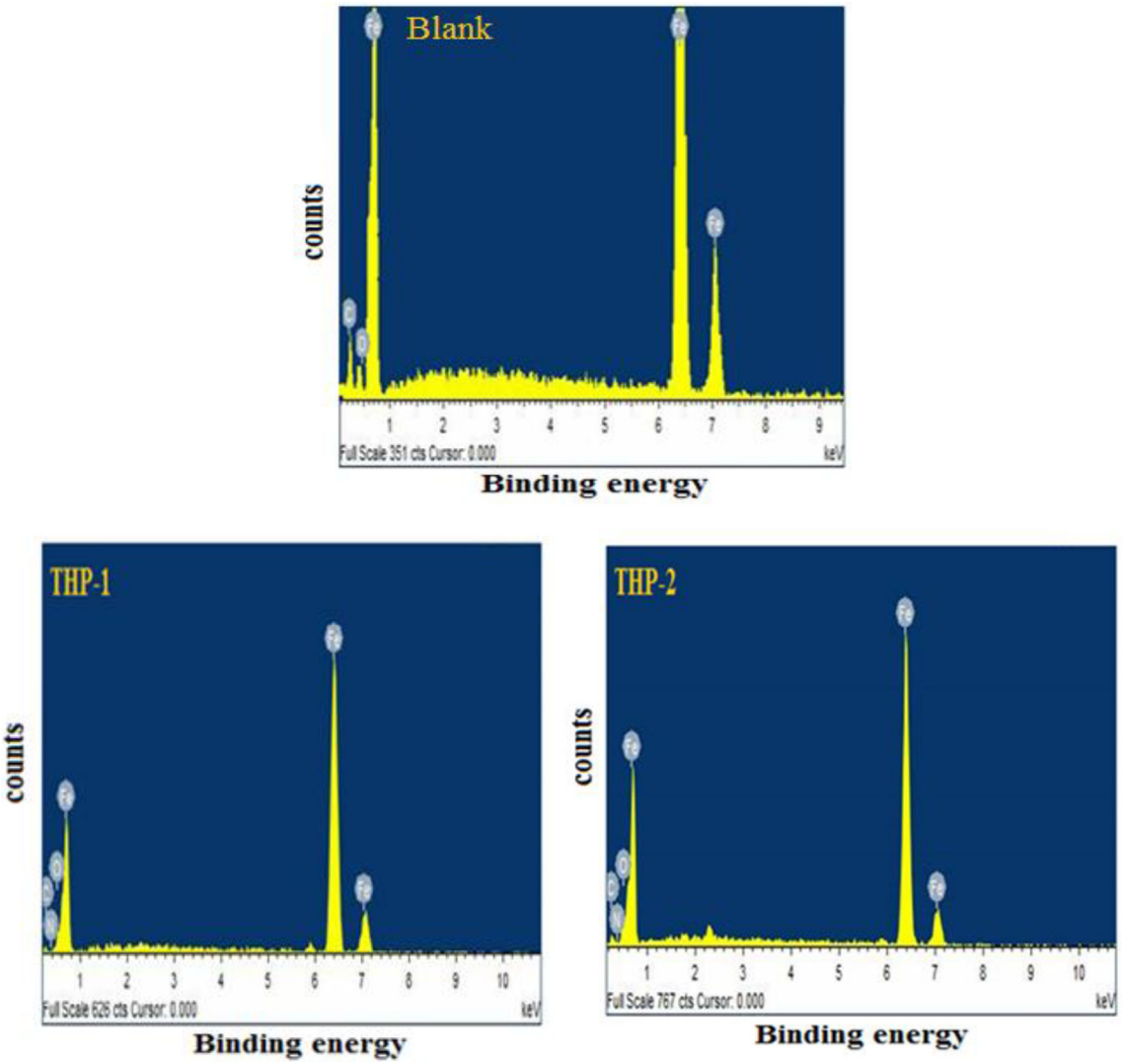

Fig. 7. EDX spectra of mild steel in absence and presence of 40 ppm of THPs inhibitors.

during SEM/EDX operation processes. Further, the EDX spectra of the metallic surface in presence of inhibitors (Fig. 7) show two additional signals corresponding to nitrogen and oxygen, which clearly reveal the presence of inhibitor on the surface.

AFM analysis

The AFM micrographs of MS specimens in absence and presence of optimum concentrations of two studied inhibitor molecules are shown in Fig. 8. From the Fig. 8 it can be seen that AFM micrograph of the MS surface shows a highly corroded and rough surface which is again attributed to free acid corrosion in acid solution with any inhibitors. The calculated average surface roughness was 580 nm. However, the AFM micrographs in presence of inhibitors show significant improvement in the metallic surface morphology. The smoothed surface morphologies of metallic surfaces in presence of studied inhibitors is resulted to the formation of a protective film by the inhibitors molecules which isolate the metals from corrosive environments. The average surface roughness's were decreased to 264 and 190 nm in presence of 7.95×10^{-5} M concentrations of THP-1 and THP-2, respectively. The high surface smoothness of metallic specimens for THP-2 as compare to THP-1 further indicates that THP-2 is comparatively more efficient corrosion inhibitors.

QC calculations

The QC calculations using DFT method has emerged as a most frequently used computational technique. These calculations provide some vital parameters, which describe the interactions between metal and inhibitors. The optimized of THP-1 and THP-2 molecules are given in Fig. 9. It is well known that in acid solution the heteroatoms (O N, S) of the organic molecule which having free lone pair of electrons get easily protonated. In our present study, we protonated the secondary amine group of both THPs molecule because it has maximum Mulliken charge −0.648 (9 N) and −0.646 (10 N) of THP-1 and THP-2, respectively (Fig. 9). Therefore, the DFT study has done of neutral as well as protonated THPs molecule in gaseous and aqueous phase and their frontier molecular electron distribution (HOMOs and LUMOs) and molecular electrostatic potential (MEP) structure are depicted in Figs. 10 and 11, respectively.

In general, E_{HOMO} of any reacting molecule is a measure of tendency to donate its non-bonding and π-electron to the appropriate accepting molecule. It can be seen that values of E_{HOMO} are increasing from going THP-1 to THP-2, which indicates that reactivity, and therefore IE increases in the same order in both gaseous (THPs-G) and aqueous (THPs-A) phases (Table 8). It can be seen that HOMO (highest occupied molecular orbital) frontier electron distribution is mostly localized over phenyl ring attached through the electron donating group (secondary

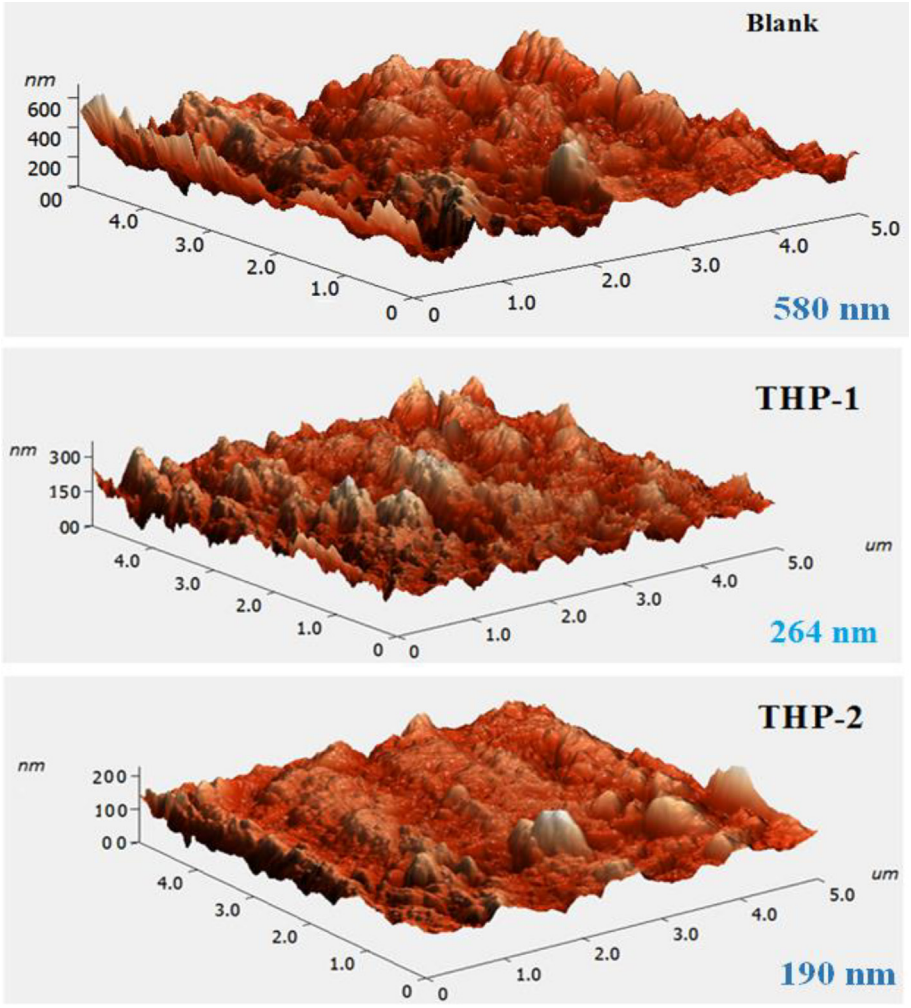

Fig. 8. AFM image of mild steel in absence and presence of 40 ppm of THPs inhibitors.

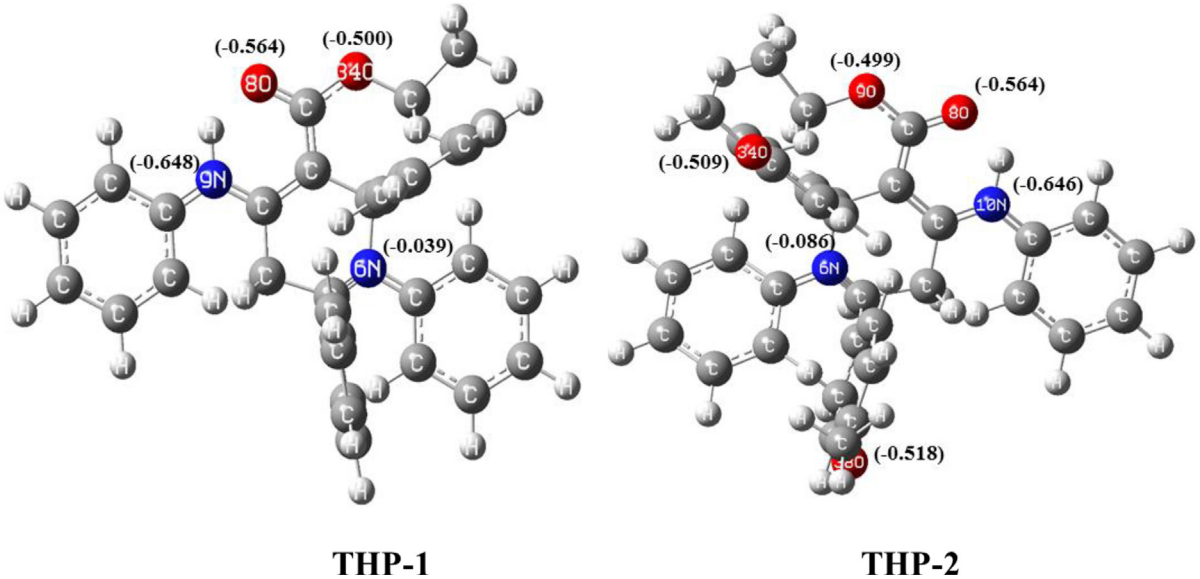

Fig. 9. Optimized molecular structure of inhibitor molecules.

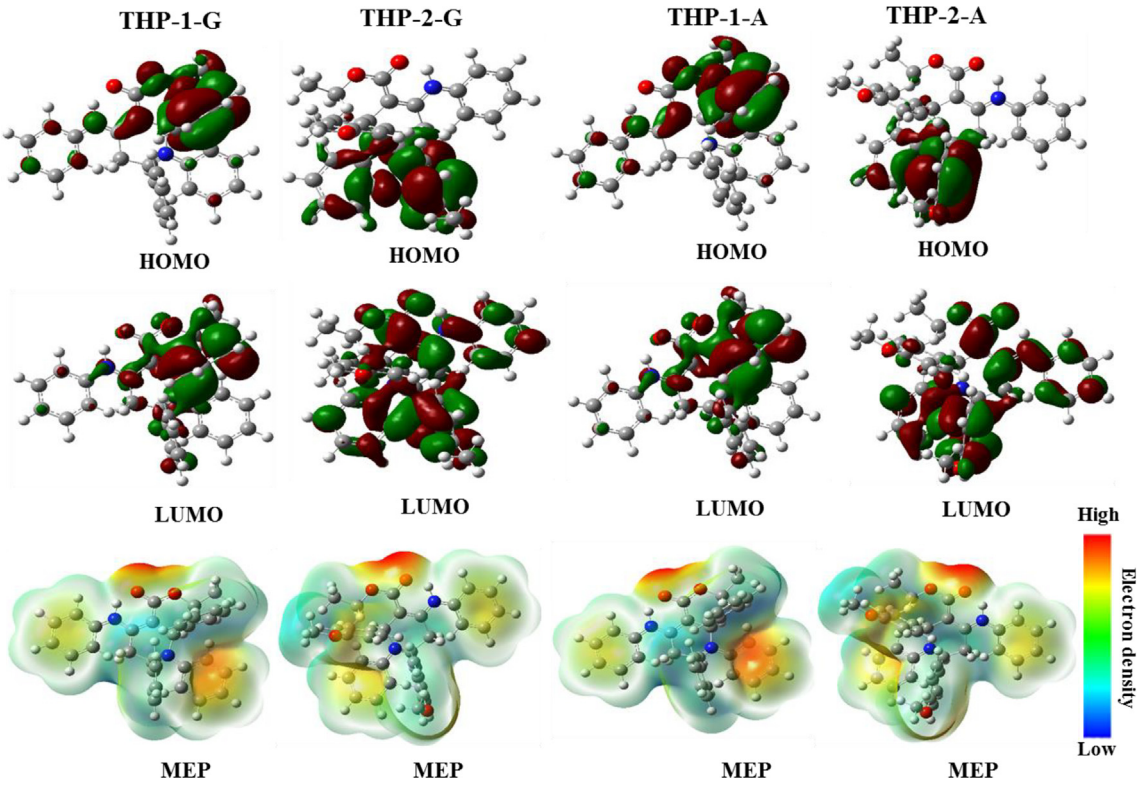

Fig. 10. The HOMOs, LUMOs and molecular electrostatic potential (MEP) of Neutral THPs inhibitors in gas (G) and in aqueous (A) phase.

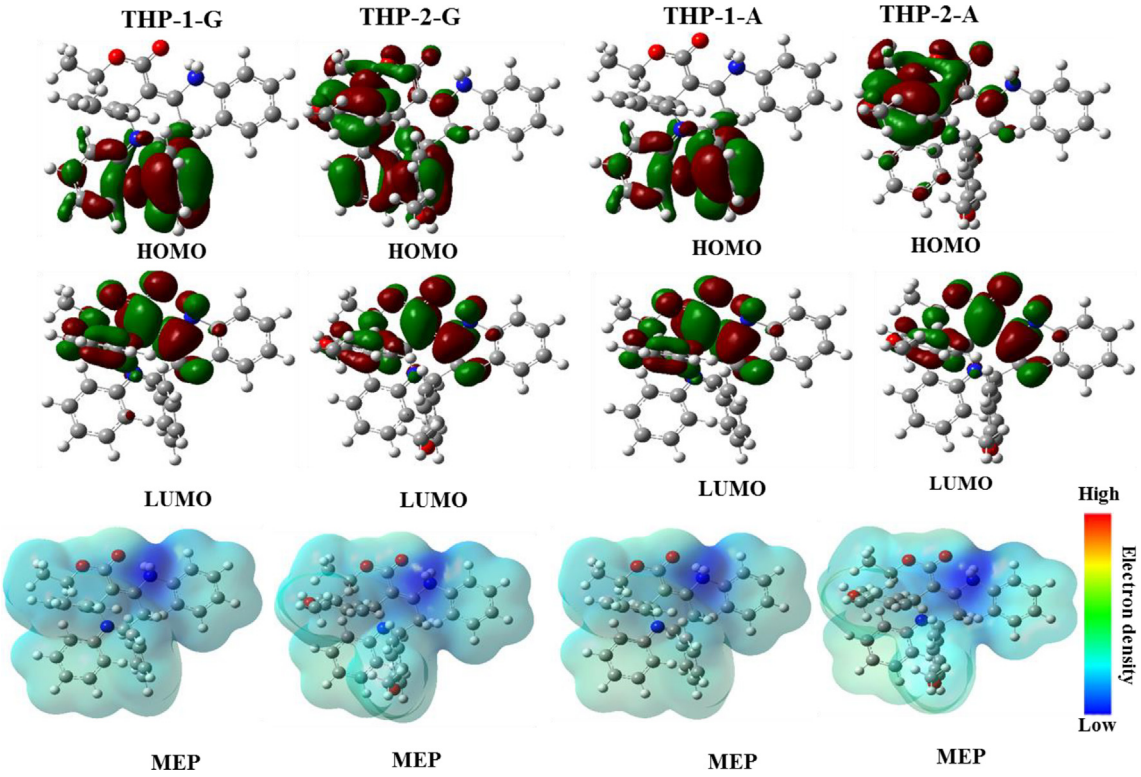

Fig. 11. The HOMOs, LUMOs and molecular electrostatic potential (MEP) of protonated THPs inhibitors in gas (G) and in aqueous (A) phase.

amine) in THP-1 molecules, while in THP-2 molecule, the HOMO distributed over the one of the phenyl ring attached through the electron donor tertiary amine and one of the methoxy substituted phenyl ring (Fig. 10). Careful observation of the frontier molecular orbitals show that the HOMOs and LUMOs are distributed almost on entire part of the molecules in both gaseous and aqueous phases (Fig. 10). However, molecular electron distribution is relatively more in the case of T-2 as compared to the THP-1 which implies that THP-2 interacts relatively more effectively as compared to the THP-1. Obviously, lower value of E_{LUMO} has associated the higher reactivity of inhibitor molecules. While

Table 8
Quantum chemical parameters derived from the B3LYP/6-31G (d, p) method.

Parameters→ Inhibitors↓		E_{HOMO} (eV)	E_{LUMO} (eV)	ΔE (eV)	η (eV)	σ (eV)	χ (eV)	ΔN_{110}	ω	ε
Neutral form										
Gaseous	THP-1	−4.17	−1.21	2.96	1.48	0.68	2.69	0.72	1.22	0.82
	THP-2	−3.77	−0.91	2.87	1.43	0.70	2.34	0.88	0.96	1.04
Aqueous	THP-1	−4.15	−1.19	2.96	1.48	0.68	2.67	0.73	1.20	0.83
	THP-2	−3.86	−0.98	2.83	1.44	0.70	2.42	0.83	1.02	0.98
Protonated form										
Gaseous	THP-1	−6.80	−5.46	1.34	0.67	1.49	6.13	−0.98	13.14	0.08
	THP-2	−7.28	−5.34	1.93	0.97	1.03	6.31	−0.77	10.26	0.10
Aqueous	THP-1	−4.43	−2.55	1.88	0.94	1.06	3.49	0.71	3.24	0.31
	THP-2	−4.69	−2.52	2.17	1.08	0.92	2.27	1.18	1.19	0.84

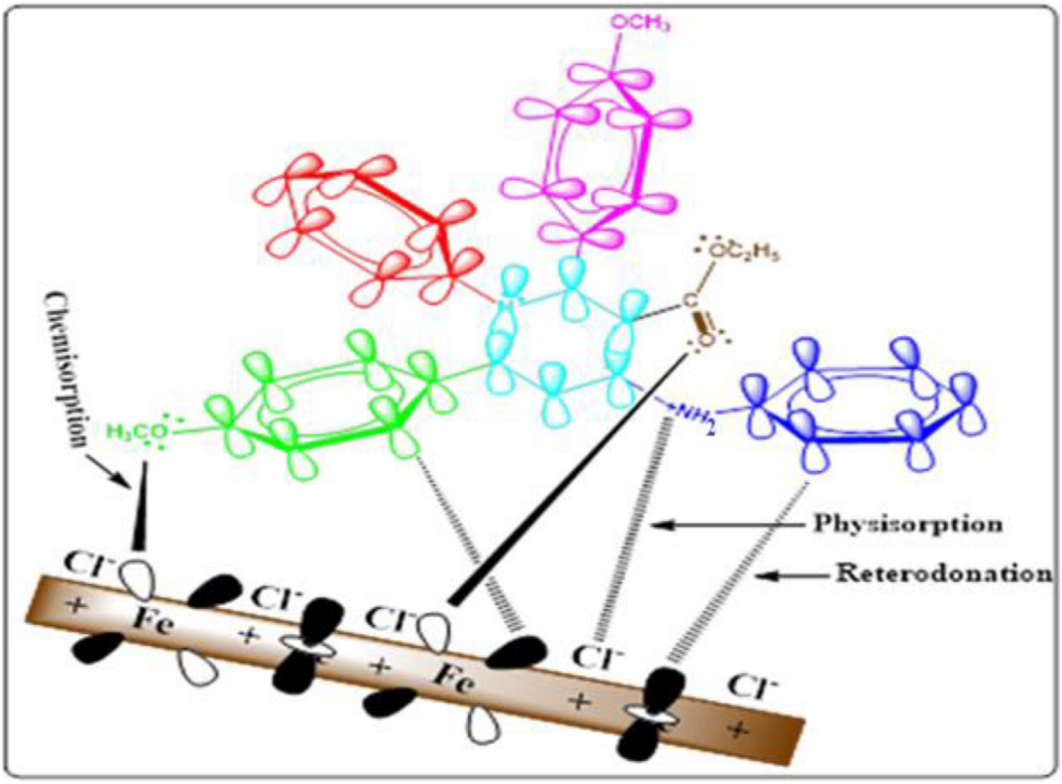

Fig. 12. Pictorial representation of adsorption of THP-2 inhibitor on mild steel surface in 1 M HCl.

the values of E_{LUMO} is listed in Table 8, did not support experimentally performance of THPs molecules, the abnormality was also find in our earlier work [47]. The reactive sites of inhibitor molecules were further confirmed by the molecular electrode potential (MEP) studies by using the B3LYP/6-13 G (d, p) basis set, shown in Fig. 10. The MEP studies of THPs molecule, red to green region is associated with electrophilic attack, are mainly observed over the oxygen and some of the phenyl carbons. While the green to blue region is associated to the nucleophilic region, which is distributed over the entire part of the THPs in both the gaseous and aqueous phase (Fig. 10). The energy band gap (ΔE) is used to describe the relative reactivity of molecules among a series. In general, a molecule with lower value of ΔE associates with high chemical reactivity and therefore should exhibit higher IE. In our present study value of ΔE follows the order: THP-2 < THP-1, which is in accordance with order of IE obtained experimentally. Further, the inhibition performance of both the inhibitor molecules was measured by determining their electronegativity. In general, lower electronegativity of inhibitor molecule having more capability to donate electrons to vacant metal orbital and vice versa. The results listed in Table 8 is showed that THP-2 has more donor tendency than THP-1. A molecule with lower value of hardness is associated with high chemical reactivity and therefore high inhibition performance. In our present study, the values of hardness follow the trends: THP-2 > THP-1 which again accordance with the order of IE obtained by experimental means. While the value of softness was just, converse to the hardness and again justified the experimental order of IE. The fraction of electron transfers which a measure of a relative amount of electron transfer from one molecule to other was also determined for both the inhibitors. The THP-2 possesses the higher positive value of fraction of electron transfer as compared to THP-1 indicating that THP-2 has comparatively higher tendency to transfer its electrons to the vacant d-orbital of Fe atoms during metal inhibitor interactions. Electrophilicity index (ω) is another parameter, which tells about the electron-accepting tendency of the inhibitors molecules, and it is just reverse of nucleophilicity index (ε) which measure the electron donor tendency [48]. From the results, it can be observed that THP-2 has higher value of ε and lower value ω than THP-1, indicated that THP-2 have greater electron donor tendency to metal as and have lesser electron acceptor capability from the metal as compared to THP-1.

Mechanism of inhibition

The adsorption mechanism of THPs inhibitor on MS surface can elucidate based on idea obtained from the experimental, surface and DFT studies. Based on PDP and best fitted Langmuir absorption result, the THPs molecule adsorbs on the MS surface through both physisorption and chemisorption mood, shown in Fig. 12. In 1 M HCl solution the amine group of THPs molecule get protonated (confirmed by QC study), which promote the electrostatic interaction with negatively charged metal created by reabsorbed Cl^- ions (physisorption). At the same time, chemisorption force created by donation of the available lone pair of electrons on heteroatoms (O, N) and π-electrons on the phenyl rings to the vacant 3d-orbitals of Fe [49]. The high reactivity of THP-2, due to presence two O-Me groups offers the extra chemisorption. In addition to this, the donation π-electrons of phenyl rings to the vacant 3d orbitals of Fe and simultaneously, its vacant antibonding π-orbitals get offers to accept electrons from filled metal orbitals (retrodonation), which provide the extra potential of THPs inhibitor to interact with mild steel [50].

Conclusion

From the weight loss, electrochemical (EIS and Tafel), surface (AFM/SEM and EDX) and QC calculations described in the present study it is concluded that: both the studied THPs act as good corrosion inhibitors for MS in 1 M HCl and their inhibition characteristics increase with concentrations. Among the studied compounds, THP-2 exhibited better IE 94.81% than THP-1 (91.19%) at the optimum concentration. EIS study revealed that investigated compounds retard corrosion through adsorbing on the metal surface. Adsorption of both inhibitors followed the Langmuir adsorption isotherm. PDP study showed that both inhibitors behaved as mixed type. SEM/EDX and AFM analyses supported the inhibition behavior of investigated inhibitors. QC calculations provide good insight about the electronic properties and the adsorption behavior of the studied molecules on the metallic surface. Experimental results were well complemented by QC calculation results.

Appendix A. Supplementary data

Supplementary data associated with this article can be found, in the online version, at http://dx.doi.org/10.1016/j.rinp.2018.04.069.

References

[1] Sasikumar Y, Adekunle AS, Olasunkanmi LO, Bahadur Baskar IR, Kabanda MM, Obot IB, Ebenso EE. Experimental, quantum chemical and Monte Carlo simulation studies on the corrosion inhibition of some alkyl imidazolium ionic liquids containing tetrafluoroborate anion on MSin acidic medium. J Mol Liq 2015;211:105–18.

[2] Verma C, Olasunkanmi LO, Obot IB, Ebenso EE, Quraishi MA. 2,4-Diamino-5-(phenylthio)-5H-chromeno[2,3-*b*]pyridine-3-carbonitriles as green and effective corrosion inhibitors: gravimetric, electrochemical, surface morphology and theoretical studies. RSC Adv 2016;6:53933–48.

[3] Khadiri, Saddik R, Bekkouche K, Aouniti A, Hammouti B, Benchat N, Bouachrine M, Solmaz R. Gravimetric, electrochemical and quantum chemical studies of some pyridazine derivatives as corrosion inhibitors for mild steel in 1 M HCl solution. J Taiwan Inst Chem Eng 2016;58:552–64.

[4] Azhar ME, Mernari M, Traisnel M, Bentiss F, Lagrenee M. Corrosion inhibition of mild steel by the new class of inhibitors [2,5-bis(n-pyridyl)-1,3,4-thiadiazoles] in acidic media. Corros Sci 2001;43:2229.

[5] Mobin M, Zehra S, Parveen M. l-Cysteine as corrosion inhibitor for mild steel in 1 M HCl and synergistic effect of anionic, cationic and non-ionic surfactants. J Mol Liq 2016;216:598–607.

[6] da Silva AB, D'Elia E, Gomes JA. Carbon steel corrosion inhibition in hydrochloric acid solution using a reduced Schiff base of ethylenediamine. Corros sci 2010;52:788–93.

[7] Verma C, Quraishi MA, Singh A. 5-Substituted 1H-tetrazoles as effective corrosion inhibitors for mild steel in 1 M hydrochloric acid. J Taibah Uni 2016;10:718–33.

[8] Abiola OK, Otaigbe JO, Kio OJ. Gossipium hirsutum L. extracts as green corrosion inhibitor for aluminum in NaOH solution. Corros Sci 2009;51:1879–81.

[9] Verma C, Olasunkanmi LO, Obot IB, Ebenso EE, Quraishi MA. 5-Arylpyrimido-[4,5-*b*]quinoline-diones as new and sustainable corrosion inhibitors for mild steel in 1 M HCl: a combined experimental and theoretical approach. RSC Adv 2016;6:15639–54.

[10] Deshmukh MB, Salunkhe SM, Patil DR, Anbhule PV. A novel and efficient one step synthesis of 2-amino-5-cyano-6-hydroxy-4-aryl pyrimidines and their anti-bacterial activity. Eur J Med Chem 2009;44:2651–4.

[11] Kappe CO. Biologically active dihydropyrimidones of the Biginelli-type-a literature survey. Eur J Med Chem 2000;35:1043–52.

[12] Ganem B. Strategies for innovation in multicomponent reaction design. Acc Chem Res 2009;42:463–72.

[13] Kumar GS, Ragini SP, Kumar AS, Meshram HM. A copper-catalyzed multi-component reaction accessing fused imidazo-heterocycles via C-H functionalization. RSC Adv 2015;5:51576–80.

[14] Mateeva NN, Winfield LL, Redda KK. The chemistry and pharmacology of tetrahydropyridines. Curr Med Chem 2005;12:551–71.

[15] Wang HJ, Mo LP, Zhang ZH. Cerium ammonium nitrate-catalyzed multicomponent reaction for efficient synthesis of functionalized tetrahydropyridines. ACS Comb Sci 2010;13:181–5.

[16] Yadav M, Kumar S, Kumari N, Bahadur I, Ebenso EE. Experimental and theoretical studies on corrosion inhibition effect of synthesized benzothiazole derivatives on mild steel in 15% HCl solution. Int J Electrochem Sci 2015;10:602–24.

[17] Khodaei-Tehrani M, Niazi A. Electrochemical and Theoretical Evaluation of 5, 5′-(Pyridine-2, 6-diyl) bis (4-phenyl-4H-1, 2, 4-triazole-3-thiol) as a Novel Corrosion Inhibitor of mild steel in the Acidic Medium. Int J Electrochem Sci 2015;10:6855–71.

[18] Gupta NK, Verma C, Quraishi MA, Mukherjee AK. Schiff's bases derived from l-lysine and aromatic aldehydes as green corrosion inhibitors for mild steel: experimental and theoretical studies. J Mol Liq 2016;215:47–57.

[19] Khan MZ, Aziz MA, Hasan MR, Al-Mamun MR. The role of drug as corrosion inhibitor for mild steel surface characterization by SEM, AFM, and FTIR. Anti-Corros Method Mater 2016;63:308–15.

[20] Becke AD. A new mixing of Hartree-Fock and local density-functional theories. J Chem Phys 1993;98:1372–7.

[21] Haque J, Ansari KR, Srivastava V, Quraishi MA, Obot IB. Pyrimidine derivatives as novel acidizing corrosion inhibitors for N80 steel useful for petroleum industry: a combined experimental and theoretical approach. J Ind Eng Chem 2017;49:176–88.

[22] Srivastava V, Haque J, Verma C, Singh P, Lgaz H, Salghi R, Quraishi MA. Amino acid based imidazolium zwitterions as novel and green corrosion inhibitors for mild steel: experimental, DFT and MD studies. J Mol Liq 2017;244:340–52.

[23] Pearson R. GInorg. Chem. 1988;27:734–40.

[24] Cao Z, Tang Y, Cang H, Xu J, Lu G, Jing W. Novel benzimidazole derivatives as corrosion inhibitors of mild steel in the acidic media. Part II: Theoretical studies. Corros Sci 2014;83:292–8.

[25] Singh A, Ansari KR, Haque J, Dohare P, Lgaz H, Salghi R, Quraishi MA. Effect of electron donating functional groups on corrosion inhibition of mild steel in hydrochloric acid: experimental and quantum chemical study. J Taiwan Ins Chem Eng. 2018;82:233–51.

[26] Parr RG, Szentpaly LV, Liu S. Electrophilicity index. J Am Chem Soci 1999;121:1922–4.

[27] Kadhim A, Al-Okbi AK, Jamil DM, Qussay A, Al-Amiery AA, Gaaz TS, Kadhum AA, Mohamad AB, Nassir MH. Experimental and theoretical studies of benzoxazines corrosion inhibitors. Results phys. 2017;7:4013–9.

[28] Behpour M, Ghoreishi SM, Soltani N, Salavati-Niasari M. The inhibitive effect of some bis-N,S-bidentate Schiff bases on corrosion behaviour of 304 stainless steel in hydrochloric acid solution. Corros Sci. 2009;51:1073–82.

[29] Rani BE, Basu BB. Green inhibitors for corrosion protection of metals and alloys: an overview. Int J Corros 2012;2012.

[30] Verma C, Quraishi MA, Olasunkanmi LO, Ebenso EE. L-Proline-promoted synthesis of 2-amino-4-arylquinoline-3-carbonitriles as sustainable corrosion inhibitors for mild steel in 1 M HCl: experimental and computational studies. RSC Adv 2015;5:85417–30.

[31] Schmid GM, Huang HJ. Spectro-electrochemical studies of the inhibition effect of 4,7-diphenyl-1,10-phenanthroline on the corrosion of 304 stainless steel. Corros Sci 1980;20:1041–57.

[32] Hameed RA, Ismail EA, Abu-Nawwas AH, Al-Shafey HI. Expired Voltaren drugs as corrosion inhibitor for aluminium in hydrochloric acid. Int J Electrochem Sci 2015;10:2098–109.

[33] Obot IB, Obi-Egbedi NO, Umoren SA. Adsorption characteristics and corrosion inhibitive properties of clotrimazole for aluminium corrosion in hydrochloric acid. Int J Electrochem Sci 2009;4:863–77.

[34] Ghareba S, Omanovic S. Interaction of 12-aminododecanoic acid with a carbon steel surface: towards the development of 'green' corrosion inhibitors. Corros Sci 2010;52:2104–13.

[35] Amin MA, Ibrahim MM. Corrosion and corrosion control of mild steel in concentrated H_2SO_4 solutions by a newly synthesized glycine derivative. Corros Sci 2011;53:873–85.

[36] Goulart CM, Esteves-Souza A, Martinez-Huitle CA, Rodrigues CJ, Maciel MA, Echevarria A. Experimental and theoretical evaluation of semicarbazones and thiosemicarbazones as organic corrosion inhibitors. Corros Sci 2013;67:281–91.

[37] Yıldız R, Doğan T, Dehri I. Evaluation of corrosion inhibition of mild steel in 0.1 M HCl by 4-amino-3-hydroxynaphthalene-1-sulphonic acid. Corros Sci 2014;85:215–21.

[38] Shukla SK, Ebenso EE. Corrosion inhibition, adsorption behavior and thermodynamic properties of streptomycin on mild steel in hydrochloric acid medium. Int J Electrochem Sci 2011;6:3277–91.

[39] Xu F, Duan J, Zhang S, Hou B. The inhibition of mild steel corrosion in 1 M

hydrochloric acid solutions by triazole derivative. Mater Lett 2008;62:4072–4.
[40] Chetouani A, Hammouti B. Salvia officinalis essential oil and the extract as green corrosion inhibitor of mild steel in hydrochloric acid. J Chem Pharm Res 2014;6:1401–16.
[41] Verma C, Olasunkanmi LO, Ebenso EE, Quraishi MA, Obot IB. Adsorption behavior of glucosamine-based, pyrimidine-fused heterocycles as green corrosion inhibitors for mild steel: experimental and theoretical studies. J Phys Chem C 2016;120:11598–611.
[42] Yıldız R. An electrochemical and theoretical evaluation of 4,6-diamino-2-pyrimidinethiol as a corrosion inhibitor for mild steel in HCl solutions. Corros Sci 2015 Jan;1(90):544–53.
[43] Gupta NK, Verma C, Salghi R, Lgaz H, Mukherjee AK, Quraishi MA. New phosphonate based corrosion inhibitors for mild steel in hydrochloric acid useful for industrial pickling processes: experimental and theoretical approach. New J Chem 2017;41:13114–29.
[44] Khaled KF, Abdel-Shafi NS, Al-Mobarak NA. Understanding corrosion inhibition of iron by 2-thiophenecarboxylic acid methyl ester: Electrochemical and computational study. Int J Electrochem Sci 2012;7:1027–44.
[45] Yousefi A, Javadian S, Dalir N, Kakemam J, Akbari J. Imidazolium-based ionic liquids as modulators of corrosion inhibition of SDS on mild steel in hydrochloric acid solutions: experimental and theoretical studies. RSC Adv 2015;5:11697–713.
[46] Asefi D, Mahmoodi NM, Arami M. Effect of nonionic co-surfactants on corrosion inhibition effect of cationic gemini surfactant. Colloids Surf A: Physicochem Eng Aspects 2010;355:183–6.
[47] Verma C, Olasunkanmi LO, Ebenso EE, Quraishi MA. Adsorption characteristics of green 5-arylaminomethylene pyrimidine-2,4,6-triones on MSsurface in acidic medium: experimental and computational approach. Results Phys 2018;8:657–70.
[48] Erdoğan Ş, Safi ZS, Kaya S, Işın DÖ, Guo L, Kaya C. A computational study on corrosion inhibition performances of novel quinoline derivatives against the corrosion of iron. J Mol Struct 2017;1134:751–61.
[49] Wan K, Feng P, Hou B, Li Y. Enhanced corrosion inhibition properties of carboxymethyl hydroxypropyl chitosan for mild steel in 1.0 M HCl solution. RSC Adv 2016;6(81):77515–24.
[50] Singh A, Ansari KR, Xu X, Sun Z, Kumar A, Lin Y. An impending inhibitor useful for the oil and gas production industry: Weight loss, electrochemical, surface and quantum chemical calculation. Sci Rep 2017;7(1):14904.